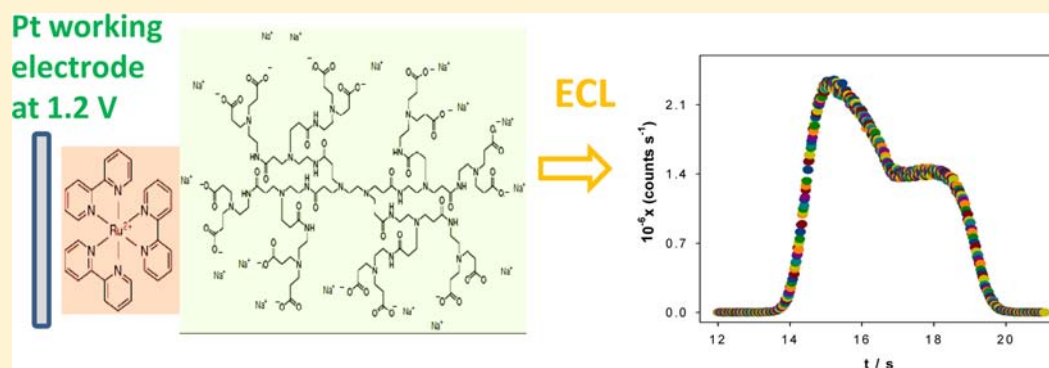


# Electrochemiluminescence of the $[\text{Ru}(\text{bpy})_3]^{2+}$ Complex: The Coreactant Effect of PAMAM Dendrimers in an Aqueous Medium

P. Perez-Tejeda,\* R. Prado-Gotor, and E. M. Grueso

Department of Physical Chemistry, Faculty of Chemistry, University of Seville, c/Profesor García González s/n, 41012 Seville, Spain

**S** Supporting Information

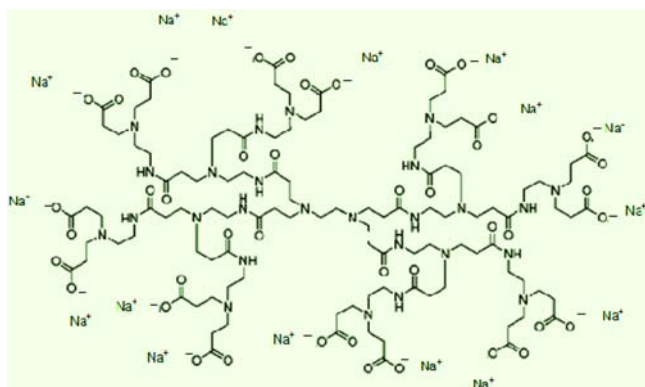


**ABSTRACT:** Electrogenerated chemiluminescence (ECL) from aqueous solutions of tris(2,2'-bipyridine)ruthenium(II),  $[\text{Ru}(\text{bpy})_3]^{2+}$ , in the presence of PAMAM G1.5 and G4.5 dendrimers, was observed without the addition of coreactants. The ECL efficiency,  $\Phi_{\text{ECL}}$ , was enhanced with the addition of increasing amounts of G1.5 dendrimer. Indeed, the ECL efficiency for the  $[\text{Ru}(\text{bpy})_3]^{2+}$ /G1.5 dendrimer became about 10 times higher than that for the  $[\text{Ru}(\text{bpy})_3]^{2+}$ /oxalate anion system. However, the ECL efficiency in the presence of the G4.5 dendrimer was smaller than that for the G1.5 dendrimer at concentrations similar to those for G1.5 with identical medium conditions. Besides, the addition of NaCl at a given concentration of G1.5 dendrimer decreased the ECL efficiency. The results of  $\Phi_{\text{ECL}}$  were interpreted by taking into account the coreactant effect and the electrostatic (long-range and short-range) interactions between the ruthenium(II) complex and the electric field of the dendrimer surface. Standard formal potentials of the  $[\text{Ru}(\text{bpy})_3]^{3+/2+}$  couple in the presence of G1.5 and G4.5 dendrimers were also determined.

## 1. INTRODUCTION

Dendritic polymers or dendrimers are macromolecules that consist of a polyfunctional core with shells of monomer units extending off branching points (see Chart 1).<sup>1</sup> These macromolecules have well-defined molecular weights and

**Chart 1. Chemical Structure of the PAMAM G1.5 Dendrimer**



end-group functionalities. Because of the way that the dendrimeric macromolecules are synthesized, it is possible to control the size, shape, structure, and surface functional groups for a desired application.<sup>2</sup> Up to now, dendrimers have been widely applied in many fields, such as host–guest chemistry, metal-ion binding, surface modifications, nanoparticle synthesis, etc.<sup>1,2</sup> Recently, dendrimers have been used as carriers of biologically and medically important molecules.<sup>1,3</sup> Special expectations are associated with the use of these polymers as carriers of oncologic drugs because this class of molecules can be transferred to dendrimers through covalent or noncovalent bonding, such as hydrogen-bonding, electrostatic, and hydrophobic interactions.<sup>4–6</sup>

Based on the foregoing, the subject of ligand–dendrimer interactions is of interest because understanding these interactions can help to address important points related to the potential applications of these unique nanomaterials. The goal of this study is to obtain a deeper insight into the dendrimer–ligand interactions using electrogenerated chem-

Received: June 11, 2012

Published: September 28, 2012

iluminescent (ECL) reactions and poly(amidoamine), i.e., the PAMAM series of starburst dendrimers.

The PAMAM series of dendrimers are some of the best-known water-soluble dendrimers, which are composed of amidoamine monomer units emanating from a central core such as ethylenediamine. The dendrimers are referred to by their generations: GX.0 and GX.5 ( $X = 0, 1, 2 \dots$ ) denoting full generation with primary amines as end groups and a half-generation terminating in carboxylic acid or carboxylate anions, respectively (see Chart 1).<sup>2</sup> In addition to the final groups, these dendrimers possess internal tertiary amines and amide groups, so that all of these functional groups can play the role of active sites capable of bonding a ligand.

Another characteristic of PAMAM dendrimers is their ability to accumulate positive charges by protonation of the primary amines or carboxylate groups at the surface and the internal tertiary amines depending on the medium pH.<sup>7,8</sup> Thus, the primary amine groups of the outer rim protonate at  $7 < \text{pH} < 8$ , whereas the tertiary amines inside the dendrimer protonate at  $2 < \text{pH} < 5$ .<sup>7,8</sup> Moreover, for the case of the half-generation dendrimers at  $3 < \text{pH} < 6$ , the tertiary amines in the interior are entirely protonated; however, a fraction of the terminal carboxylate groups remain without being protonated.<sup>9</sup> That is, half-generation dendrimers can become a unique system possessing positive charges inside and negative charges outside,<sup>10</sup> so they can behave as zwitterions at the 3–6 pH range.

Additionally, optical absorption and photochemistry measurements using small charged molecules as probes detected structural changes from lower to higher generations. Thus, dendrimers of generations G2.5 or less have an open and flexible structure, whereas those of G3.5 and higher have a more rigid and spherical structure.<sup>11</sup> Similarly, changes of the pH medium may originate alterations in the structures of dendrimers, going from a dense-shell to a dense-core structure when the pH increases.<sup>12</sup> Consequently, the operability of the active sites as the structure of dendrimers can be a function of the medium pH, so it is convenient to work at a fixed pH (vide infra).

Many studies have been carried out on ECL systems containing chelates of ruthenium(II),<sup>13–15</sup> which yield characteristic emission spectra from the triplet metal-to-ligand charge-transfer (MLCT) excited state of ruthenium(II) chelates. This generation of the  $\text{Ru}^{\text{II}*}$  excited state can be performed via the direct annihilation of ruthenium(I) and ruthenium(III) complexes in cyclic potential step experiments<sup>13,14</sup> or via creation of the excited state in a single potential step in the presence of a coreactant that generates a strong oxidant or reductant intermediate<sup>13–16</sup> (see schemes in refs 13, 14, and 16 for details). That is, the imposition of a suitable electrical signal to the working electrode causes light emission. High sensitivity and selectivity in ECL detection are due to the specific nature of the ECL reaction that controls both electrochemical and spectroscopic variables,<sup>13–16</sup> ECL has become a more sensitive and selective method than photoluminescence to detect microscopic interactions.

Besides, the study of ECL reactions in the presence of PAMAM dendrimers has recently been of interest as templates for the preparation of new sensors and quantum dots (QDs).<sup>17</sup> That is, PAMAM dendrimers together with polypyridylruthenium(II) complexes or QDs, are the basis of selective ECL sensors and biosensors.<sup>17</sup> So, dendrimers bearing complexes of ruthenium(II) as end groups increase the ECL

intensity in relation to that of the monomeric ruthenium(II) complex; however, tripropylamine<sup>17a–d</sup> as a coreactant in acetonitrile<sup>17b,c</sup> or nonionic surfactant<sup>17a</sup> or aqueous dimethylformamide/dimethyl sulfoxide<sup>17d</sup> solutions were used. In addition, the nanoclusters formed inside dendrimers are excellent systems for studies of the quantum size effects and, moreover, these dendrimer QDs have proven to be excellent ECL biosensors for analytical diagnostics<sup>17e,f</sup> and for assays in cancer cells.<sup>17g–i</sup> Another strategy for the preparation of ECL biosensors is the use of nanoparticles functionalized with polypyridylruthenium(II) complexes in the presence of PAMAM dendrimers<sup>17j</sup> or the well use of dendrimers functionalized with ruthenium(II) complexes in the presence of a thin layer of single-wall carbon nanotubes,<sup>17k</sup> which have demonstrated to be highly sensitive and selective for immunoglobulin G detection<sup>17j</sup> and for mercury-ion recognition in specific oligonucleotides.<sup>17k</sup> Nevertheless, for all of these cases, peroxydisulfate anion,<sup>17e–i</sup> tripropylamine,<sup>17k</sup> and oxalate anion<sup>17j</sup> were also used as coreactants.

In this work, dendrimer–ligand interactions have been studied using ECL reactions. Aqueous solutions containing tris(2,2'-bipyridine)ruthenium(II)  $\{[\text{Ru}(\text{bpy})_3]^{2+}\}$ , NaCl, and PAMAM dendrimers of half-generation (G1.5 and G4.5) were utilized. A  $0.1 \text{ mol dm}^{-3}$  buffer  $\text{Na}_2\text{PO}_4\text{H}/\text{NaPO}_4\text{H}_2$  (pH 6.1) was also used in order to set the structure and protonation of the dendrimers according to the preceding discussion. The remarkable find was that, besides the ligand–dendrimer interaction, G1.5 and G4.5 dendrimers behaved as coreactants, and to our knowledge, the action of PAMAM dendrimers as coreactants in ECL studies had not yet been reported.

## 2. EXPERIMENTAL SECTION

**2.1. Materials.** All chemicals [ $\text{NaCl}$ ,  $\text{Na}_2\text{C}_2\text{O}_4$ ,  $\text{Na}_2\text{PO}_4\text{H}$ ,  $\text{NaPO}_4\text{H}_2$ ,  $[\text{Ru}(\text{bpy})_3]\text{Cl}_2$ , PAMAM (ethylenediamine core), and G1.5 and G4.5 dendrimers] were analytical grade, were purchased from Sigma-Aldrich, and were used without further purification. All of the solutions were prepared with deionized water from a Millipore Milli-Q system, having a conductivity  $< 10^{-6} \text{ S m}^{-1}$ . All dendrimers were dissolved in deionized water after evaporation of methanol from the commercial sample by passing a stream of pure nitrogen through it.

**2.2. ECL Measurements.** ECL measurements were carried out with a potentiostat/galvanostat (Biologic SP-50), together with a Photon Technology International (PTI) fluorescence spectrometer; MicroBeam SA assembled, mounted, and synchronized both instruments. Thus, the voltammograms and ECL emissions were recorded simultaneously. A PC interfaced to this set of instruments allowed for the reading and handling of voltammograms and ECL emissions using *EC-Lab Express* and *Felix32* softwares, respectively.

These ECL measurements were performed in a spectroelectrochemical cell (depth = 1 cm) using a three-microelectrode array consisting of surface platinum as the working electrode, Ag/AgCl ( $3 \text{ mol dm}^{-3} \text{ NaCl}$ ) as the reference electrode, and a platinum wire as the counter electrode. A Peltier system interfaced to a set of instruments maintained the temperature constant at  $298.15 \pm 0.01 \text{ K}$  inside the cell. The microelectrodes and the Peltier system were also purchased from MicroBeam SA. The working electrode was cleaned before each ECL measurement by polishing with micrometer alumina, followed by rinsing with water, sonication in dilute nitric acid, and rinsing again twice with deionized water.

All ECL measurements were recorded using the cyclic voltammetry (CV) technique. Once the instruments and the measuring methods were calibrated, relative ECL efficiencies ( $\Phi_{\text{ECL}}$ ) were determined from the average of the two or three measurements of four scans; the uncertainty of  $\Phi_{\text{ECL}}$  measured in such a way was less than 4%. We used, as a standard,  $\Phi_{\text{ECL}}^\circ(293.15 \text{ K}) = 0.020$ ,<sup>16</sup> the reaction that

occurs between the species  $[\text{Ru}(\text{bpy})_3]^{2+}$  and  $\text{C}_2\text{O}_4^{2-}$  at 293.15 K in aqueous solutions containing  $0.1 \text{ mol dm}^{-3}$  (pH 6.1) buffer  $\text{Na}_2\text{HPO}_4/\text{NaH}_2\text{PO}_4$  and  $0.1 \text{ mol dm}^{-3}$  NaCl (ionic strength =  $0.234 \text{ mol dm}^{-3}$ ). Using the same conditions (buffer, supporting electrolyte, and reactant concentrations  $1.0 \times 10^{-4}$  and  $2.0 \times 10^{-3} \text{ mol dm}^{-3}$  for the ruthenium(II) complex and sodium oxalate, respectively),  $\Phi_{\text{ECL}}$  at 298.15 K was obtained, with its value being 0.0185, which is in agreement with the temperature influence on the ECL efficiency;<sup>18</sup> this value was taken as a reference for all relative ECL efficiency determinations. Besides, an ECL measurement was done in the absence of NaCl (ionic strength =  $0.134 \text{ mol dm}^{-3}$ ) and gave the value of  $\Phi_{\text{ECL}} = 0.0173$ , which is in agreement with the ionic strength influence on the ECL efficiency for this class of reactions.<sup>16,19</sup> Furthermore, a set of measurements was performed by changing the scan rate from  $0.5$  to  $2.0 \times 10^3 \text{ mV s}^{-1}$ , yielding similar values for the ECL efficiency (experimental uncertainty, about 4%). Also, an increase in the ruthenium(II) complex concentration up to  $1.0 \times 10^{-3} \text{ mol dm}^{-3}$  gives rise to a value equal to 0.0190 for  $\Phi_{\text{ECL}}$ , a value similar to that for the ruthenium(II) complex concentration  $1.0 \times 10^{-4} \text{ mol dm}^{-3}$ .

**2.3. Electrochemical Measurements.** Formal standard potentials,  $E^{\circ'}$ , of the  $[\text{Ru}(\text{bpy})_3]^{3+/2+}$  couple in several dendrimer solutions were determined at  $298.15 \pm 0.01 \text{ K}$  by CV and differential pulse voltammetry (DPV) techniques using a potentiostat/galvanostat (Biologic SP-50). The experimental conditions were identical with those corresponding to ECL measurements (vide supra). The system was calibrated by measuring the voltammogram of the  $[\text{Ru}(\text{bpy})_3]^{3+/2+}$  couple at  $293.15 \pm 0.01 \text{ K}$  in the same conditions as those of ref 16b. The value obtained for  $E^{\circ'}$  at  $293.15 \pm 0.01 \text{ K}$  was  $1.262 \text{ V}$  (vs SEH), almost identical with that of ref 16b.

**2.4. Spectroscopic Measurements.** Absorption and emission spectra of  $[\text{Ru}(\text{bpy})_3]^{2+}$  species were obtained by employing a Cary 500 scan UV-vis-NIR spectrophotometer and PTI fluorescence spectrometer, respectively, at  $298.15 \pm 0.01 \text{ K}$  in some dendrimer solutions in the same conditions as those corresponding to ECL measurements (vide supra). Nevertheless, no changes of the intensity or position were observed in either of the MLCT absorption and emission bands of the  $[\text{Ru}(\text{bpy})_3]^{2+}$  complex in the dendrimer solutions in relation to those in water.

### 3. RESULTS

**3.1. ECL.** All ECL measurements were recorded using the CV technique. Figure 1 shows an ECL spectrum in the presence of a G1.5 dendrimer solution (as an example) that is identical with that of photoluminescence; that is, the excited-

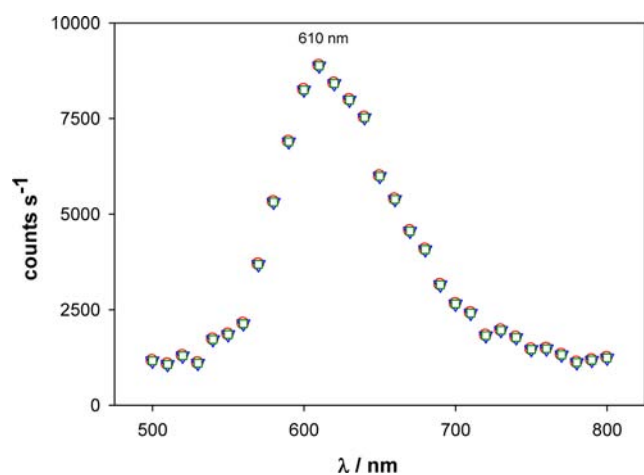


**Figure 1.** ECL spectrum in the presence of  $4.60 \times 10^{-4} \text{ mol dm}^{-3}$  G1.5 dendrimer:  $0.1 \text{ mol dm}^{-3}$  phosphate buffer (pH 6.1) +  $0.1 \text{ mol dm}^{-3}$  NaCl. Scan rates ( $\text{mV s}^{-1}$ ): red circles, 10.0; blue triangles, 5.0; green squares, 2.5.

state species generated via ECL is  $[\text{Ru}(\text{bpy})_3]^{2+*}$ . In order to obtain the ECL efficiency, however, it is more convenient to record ECL emission as a function of time.

Figure 2 shows a cyclic voltammogram (a) and its corresponding current–time curve (b) for a  $[\text{Ru}(\text{bpy})_3]^{3+/2+}$  couple in the presence of a G1.5 dendrimer solution. Also, this figure exhibits an ECL intensity–potential curve (c) and its corresponding ECL intensity–time curve (d) for a  $[\text{Ru}(\text{bpy})_3]^{2+*}$  excited state generated via CV. Thus, the full correspondence between the ECL emissions as a function of time and as a function of the potential can be observed. Additionally, a cyclic voltammogram for the  $[\text{Ru}(\text{bpy})_3]^{3+/2+}$  couple in the presence of an oxalate anion without any dendrimer is included in Figure S1a (see the Supporting Information). A comparison between both cyclic voltammograms (Figure 2a and Figure S1a in the Supporting Information) shows that dendrimer solutions have the same behavior as oxalate anion solutions. Besides, background experiments were done for all cases. In these experiments, the ECL emission was insignificant (see Figure S1b in the Supporting Information). Once the ECL emission–time and current–time curves corresponding to a given cyclic voltammogram are obtained, the ECL efficiency values can be determined. Of course, the current–time curves of the backgrounds were taken into account for calculating the ECL efficiency values.

The ECL emission efficiency, i.e., the probability of emission per charge-transfer event, can be approximately defined by the coulometric efficiency ( $\Phi_{\text{ECL}}$ ) as:<sup>20,21</sup>

$$\Phi_{\text{ECL}} = \frac{\int_0^t I \, dt}{\int_0^t i \, dt (N_A/F)} \quad (1)$$

where  $I$  and  $i$  are the intensity in photons per second and the current in amperes (coulombs per second), respectively, integrated over a finite period of time,  $t$ .  $F$  and  $N_A$  are the Faraday and Avogadro constants, respectively. Often, however, a standard reaction is used:<sup>13,21</sup>

$$\Phi_{\text{ECL}} = \Phi_{\text{ECL}}^{\circ} \frac{Q^{\circ}}{Q} \frac{I}{I^{\circ}} \quad (2)$$

with  $Q^{\circ}$  and  $Q$  being the charges passed (in coulombs) into solutions for standard and actual reactions, respectively,  $I^{\circ}$  and  $I$  the measured integrated photon intensities of solutions corresponding to the standard and actual reactions, respectively, and  $\Phi_{\text{ECL}}^{\circ}$  the ECL efficiency associated with a standard reaction. Further,  $\Phi_{\text{ECL}}$ , the coulometric efficiency, is related to  $\Phi_{\text{es}}$ , the quantum yield of excited-state formation, by:<sup>21,22</sup>

$$\Phi_{\text{es}} = \frac{\Phi_{\text{ECL}}}{\Phi_{\text{em}}} \quad (3)$$

with  $\Phi_{\text{em}}$  being the characteristic photoluminescent quantum yield of the excited-state species generated via ECL. In addition,  $\Phi_{\text{es}}$  is a relationship among homogeneous rate constants corresponding to a global mechanism of ECL.<sup>21,22</sup> Consequently, if  $\Phi_{\text{em}}$  does not change,  $\Phi_{\text{ECL}}$  must also be unchanged when the scan rate or concentration of the controlling reactant is varied. Accordingly,  $\Phi_{\text{ECL}}$  is a measure of the rate reaction leading to the luminescent state in relation to all those rates of the homogeneous reactions involved in a given ECL mechanism.

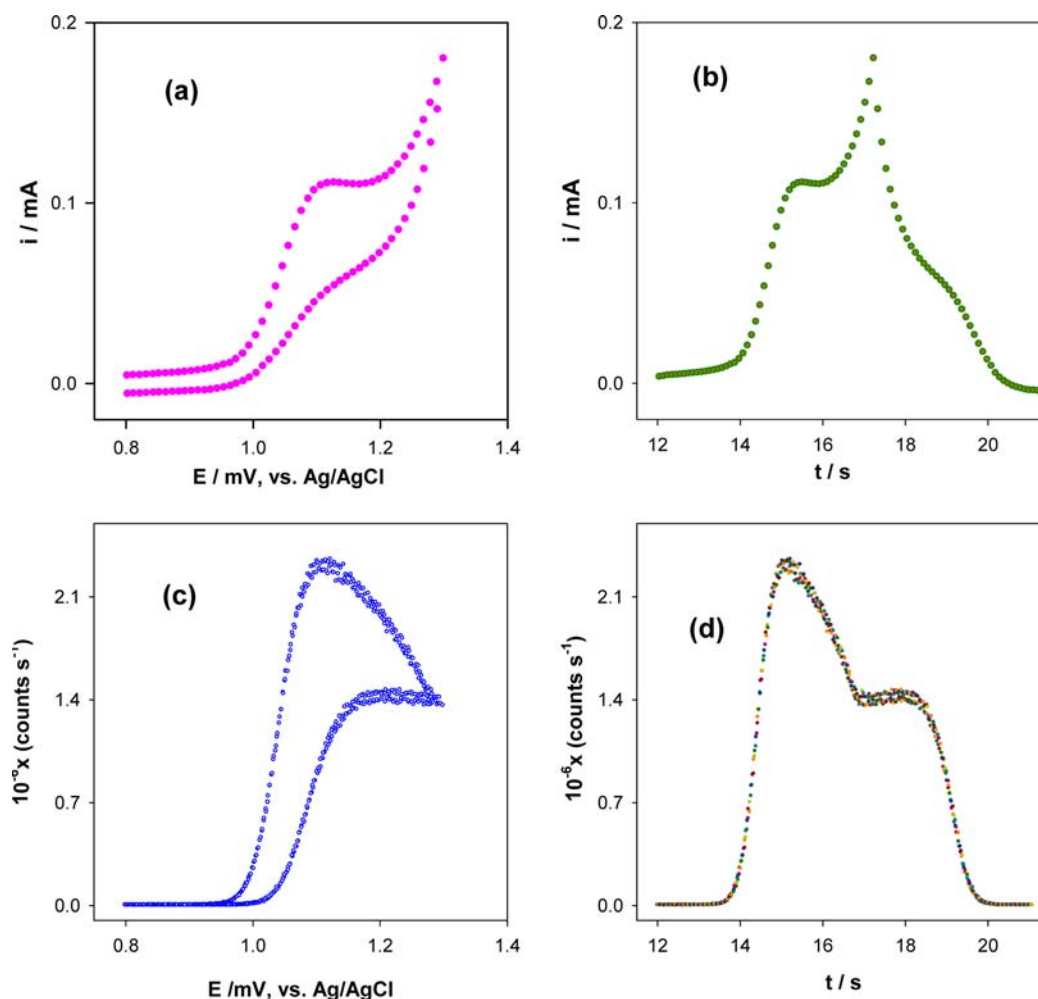


**Figure 2.** Current as a function of the potential (a) and time (b) (second scan). ECL intensity as a function of the potential (c) and time (d) (second scan) for  $[\text{Ru}(\text{bpy})_3]^{2+}$  in the presence of  $1.20 \times 10^{-4} \text{ mol dm}^{-3}$  G1.5 dendrimer without  $\text{C}_2\text{O}_4^{2-}$ :  $0.1 \text{ mol dm}^{-3}$  phosphate buffer (pH 6.1) +  $0.1 \text{ mol dm}^{-3}$  NaCl. Scan rate:  $100 \text{ mV s}^{-1}$ .

Using eqs 1 and 2, the relative ECL efficiency was determined in each medium at  $298.15 \pm 0.01 \text{ K}$ ; the results are given in Table 1. We used, as a standard, the reaction that occurs between the species  $[\text{Ru}(\text{bpy})_3]^{2+}$  and  $\text{C}_2\text{O}_4^{2-}$  (see

**Table 1. Relative ECL Efficiencies  $\Phi_{\text{ECL}}$  for Several Solutions of G1.5 and G4.5 Dendrimers at  $[\text{Na}^+] = 0.216 \text{ mol dm}^{-3}$  and for Solutions Containing Different  $[\text{Na}^+]$  at  $[\text{G1.5}] = 4.60 \times 10^{-4} \text{ mol dm}^{-3}$  ( $[\text{G1.5}]$ ,  $[\text{G4.5}]$ , and  $[\text{Na}^+]$  in  $\text{mol dm}^{-3}$ )**

$10^4[\text{G1.5}]^a$	$10^1\Phi_{\text{ECL}}^a$	$[\text{Na}^+]^b$	$10^1\Phi_{\text{ECL}}^b$
0.00	0.185	0.116	1.73
0.0310	0.230	0.216	1.66
0.398	0.650	0.616	1.55
0.698	1.02	0.916	0.905
1.20	1.41	1.216	0.160
2.46	1.46	$10^4[\text{G4.5}]^c$	$10^1\Phi_{\text{ECL}}^c$
3.59	1.48	1.13	0.910
4.60	1.66	2.30	0.414
8.30	1.80		

<sup>a</sup>Values for G1.5 dendrimer at  $[\text{Na}^+] = 0.216 \text{ mol dm}^{-3}$ . <sup>b</sup>Values for  $[\text{G1.5}] = 4.60 \times 10^{-4} \text{ mol dm}^{-3}$  in solutions containing different  $[\text{Na}^+]$ . <sup>c</sup>Values for G4.5 dendrimer at  $[\text{Na}^+] = 0.216 \text{ mol dm}^{-3}$ .

section 2.2). Furthermore, in order to establish the effect of the temperature and ionic strength on  $\Phi_{\text{ECL}}$ , some preliminary experiments were also performed. In addition, a set of measurements by changes of the scan rate or ruthenium(II) complex concentration were done. As can be seen in section 2.2, no significant change in the  $\Phi_{\text{ECL}}$  values was observed. All of these results are consistent with the physical meaning of  $\Phi_{\text{ECL}}$  previously indicated (vide supra).

In order to obtain  $\Phi_{\text{ECL}}$  values in the presence of dendrimers (Table 1), we have assumed that two electrons are transferred per dendrimer molecule to generate light emission, just as Xue Bo et al. found for ECL in the presence of aminocarboxylic acids,<sup>23</sup> in the same way as that for the case of the standard reaction,  $[\text{Ru}(\text{bpy})_3]^{2+} + \text{C}_2\text{O}_4^{2-}$  (see ref 16b). As is shown in Table 1, in the presence of solutions with changing G1.5 dendrimer concentration and in those containing G4.5 dendrimers, the  $[\text{Na}^+]_{\text{total}}$  coming from NaCl and from the buffer was  $0.216 \text{ mol dm}^{-3}$ . Another set of measurements was performed at constant concentration of the G1.5 dendrimer by adding increasing amounts of NaCl in such a way that  $[\text{Na}^+]_{\text{total}}$  ranged from 0.116 to  $1.216 \text{ mol dm}^{-3}$ .

**3.2. Standard Formal Potentials.** With the purpose of checking whether electrostatic interactions of  $[\text{Ru}(\text{bpy})_3]^{2+}$  species with the negatively charged surface of the G1.5 and G4.5 dendrimers could be operative, the redox potentials of the

$[\text{Ru}(\text{bpy})_3]^{3+/2+}$  couple in several dendrimer solutions were also determined. Table 2 shows these results at  $298.15 \pm 0.01$  K;

**Table 2.** Standard Formal Potentials versus SEH,  $E^{\circ'}$ , for Several Solutions of G1.5 and G4.5 Dendrimers at  $[\text{Na}^+] = 0.216 \text{ mol dm}^{-3}$  and for Solutions Containing Different  $[\text{Na}^+]$  at  $[\text{G1.5}] = 4.60 \times 10^{-4} \text{ mol dm}^{-3}$  ( $[\text{G1.5}]$ ,  $[\text{G4.5}]$ , and  $[\text{Na}^+]$  in  $\text{mol dm}^{-3}$ )

$10^4[\text{G1.5}]^a$	$E^{\circ'}/\text{V}^a$	$[\text{Na}^+]^b$	$E^{\circ'}/\text{V}^b$
0.00	1.272	0.116	1.343
0.0310	1.256	0.216	1.312
0.398	1.241	0.616	1.279
0.698	1.274	0.916	1.272
1.20	1.272	1.216	1.268
2.46		$10^4[\text{G4.5}]^c$	$E^{\circ'}/\text{V}^c$
3.59	1.278	1.13	1.308
4.60	1.312	2.30	1.319
8.30	1.310		

<sup>a</sup>Values for G1.5 dendrimer at  $[\text{Na}^+] = 0.216 \text{ mol dm}^{-3}$ . <sup>b</sup>Values for  $[\text{G1.5}] = 4.60 \times 10^{-4} \text{ mol dm}^{-3}$  in solutions containing different  $[\text{Na}^+]$ . <sup>c</sup>Values for G4.5 dendrimer at  $[\text{Na}^+] = 0.216 \text{ mol dm}^{-3}$ .

the value of the standard formal potential  $E^{\circ'}$  in the absence of oxalate and dendrimers was obtained by using the CV technique, and it is in agreement with other published data.<sup>24</sup> However, in the presence of dendrimer solutions at  $1.0 \times 10^{-4} \text{ mol dm}^{-3}$  of the ruthenium(II) complex, the cathodic currents were small, and for practical reasons, the DPV technique was used for evaluating  $E^{\circ'}$ . Figure 3 shows a typical differential pulse voltammogram.

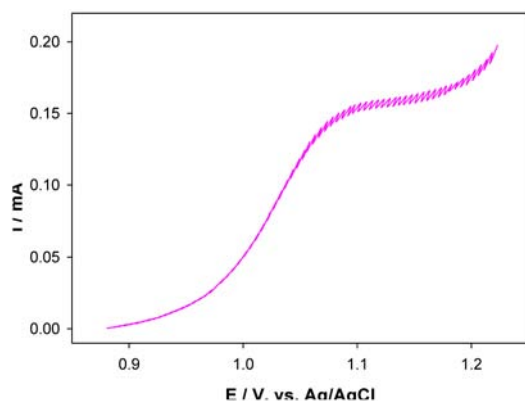


**Figure 3.** Differential pulse voltammogram for the  $[\text{Ru}(\text{bpy})_3]^{3+/2+}$  couple in  $4.60 \times 10^{-4} \text{ mol dm}^{-3}$  G1.5 dendrimer:  $0.1 \text{ mol dm}^{-3}$  phosphate buffer (pH 6.1) +  $0.8 \text{ mol dm}^{-3}$  NaCl.

The relationship between the peak and half-wave potentials for a reversible system is given by<sup>25</sup>

$$E_{\text{peak}} = E_{1/2} + \Delta E/2 \quad (4)$$

where  $\Delta E$  is the voltage amplitude of the pulse (2.5 mV in our experiments); thus,  $E_{\text{peak}} \approx E_{1/2}$ . The uncertainty in the redox potentials is about  $\pm 3$  mV.

#### 4. DISCUSSION

Figure 4 shows the ECL emission as a function of time in the absence (a) and presence (b) of G1.5 dendrimer. The remarkable thing is that you do not need the addition of an

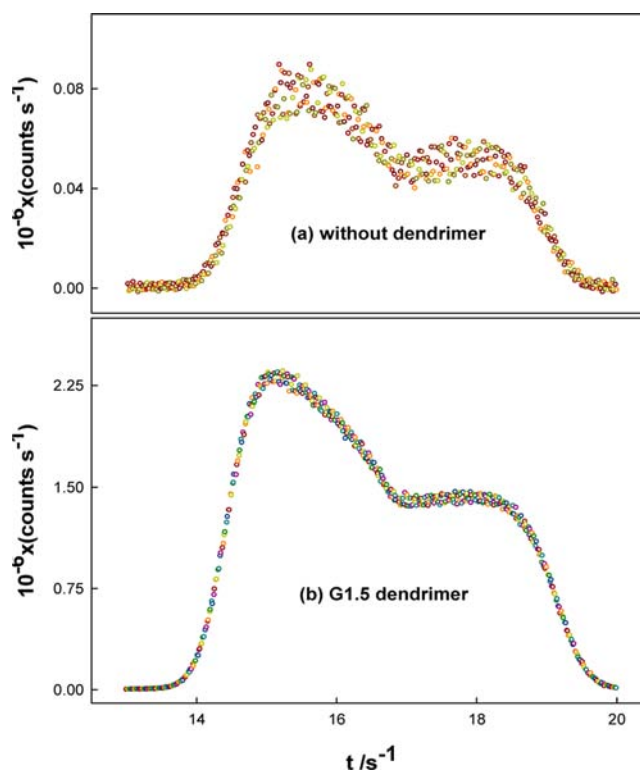


**Figure 4.** ECL intensities as a function of time (second scan) for (a) the  $[\text{Ru}(\text{bpy})_3]^{2+} + \text{C}_2\text{O}_4^{2-}$  reaction in the absence of dendrimers and (b)  $[\text{Ru}(\text{bpy})_3]^{2+}$  in the presence of  $3.59 \times 10^{-4} \text{ mol dm}^{-3}$  G1.5 dendrimer without  $\text{C}_2\text{O}_4^{2-}$ .  $0.1 \text{ mol dm}^{-3}$  phosphate buffer (pH 6.1) +  $0.1 \text{ mol dm}^{-3}$  NaCl. Scan rate:  $100 \text{ mV s}^{-1}$ .

oxalate anion to produce ECL in the presence of a dendrimer solution. Given that, both ECL–time curves have similar shapes, although for ECL emission (b) the light intensity is about 26 times higher than that for ECL emission (a), we suppose that the end carboxylate groups of the dendrimer are responsible for the ECL of the ruthenium(II) complex without the addition of an oxalate anion as the coreactant.<sup>26</sup> That is, the dendrimer itself is a coreactant. This idea is supported by the fact that the addition of increasing amounts of G1.5 dendrimer at  $[\text{Na}^+] = 0.216 \text{ mol dm}^{-3}$  increases the ECL efficiency (see Table 1). However, a linear relationship between  $\Phi_{\text{ECL}}$  and the G1.5 dendrimer concentration does not exist. Indeed, the addition of G4.5 dendrimer at concentrations similar to those for G1.5 produces an ECL efficiency diminution (see Table 1), which is surprising because G4.5 dendrimers bear more end groups than G1.5 dendrimers. Therefore, another effect must exist between the ruthenium(II) complex and the G1.5 dendrimer.

For the case of half-generation dendrimers, in line with section 1, the tertiary amines in the interior are entirely protonated, whereas a fraction of the terminal carboxylate groups remains without being protonated at pH 6.1.<sup>9</sup> Thus, on the average, the anionic species,  $\text{PO}_4\text{H}^{2-}$ ,  $\text{PO}_4\text{H}_2^-$ , and  $\text{Cl}^-$ , in the medium basically bind to the positively charged interior, whereas the cationic species,  $[\text{Ru}(\text{bpy})_3]^{2+}$  and  $\text{Na}^+$ , interact with the end carboxylate groups. Hence, an electrostatic binding of  $[\text{Ru}(\text{bpy})_3]^{2+}$  species with the electric field arising from a negatively charged surface of the G1.5 dendrimer could be operative.<sup>2,11,27</sup> Accordingly, it has been pointed out that  $E^{\circ'}$  values of the couples show a negative shift<sup>28,29</sup> when the concentrations of macromolecular receptor increase if the

electrostatic interactions between the oxidized and reduced forms of the redox couple with the receptor are effective:

$$E_b^{o'} - E_f^{o'} = 0.0592 \log \left( \frac{K_{2+}}{K_{3+}} \right) \quad (5)$$

where the subscripts b and f refer to fully bound and free probes and  $K_{2+}$  and  $K_{3+}$  are the binding constants of the reduced and oxidized species of the couple, respectively. With the purpose of checking this question, the redox potentials of the  $[\text{Ru}(\text{bpy})_3]^{3+/2+}$  couple in several dendrimer solutions were determined. From Table 2, it can be seen that both negative and positive shifts for the redox potentials of the  $[\text{Ru}(\text{bpy})_3]^{3+/2+}$  couple are found: a minimum value of  $E^{o'}$  is attained at  $3.98 \times 10^{-5} \text{ mol dm}^{-3}$  G1.5 dendrimer, whereas a positive shift is reached for the G4.5 dendrimer. The negative shift is in agreement with predictions taking into account electrostatic long-range interactions for binding,<sup>28,29</sup> in such a way that one expects a greater stabilization of the oxidized form of the couple, that is,  $K_{3+} > K_{2+}$ . Nevertheless, a positive shift of the  $E^{o'}$  values at higher concentrations of G1.5 dendrimer is also observed as previously indicated. This positive shift can be explained by considering that the  $[\text{Ru}(\text{bpy})_3]^{2+}$  species are preferentially placed on the dendrimer surface. On this surface, the strong electric field causes a sharp decrease of the solvent dielectric constant as a consequence of the dielectric saturation effects.<sup>30–32</sup> This decrease produced a decrease of both binding constants,  $K_{3+}$  and  $K_{2+}$ , but more marked in  $K_{3+}$  because it corresponds to a species with a higher charge. That is, the increase in the redox potentials of the  $[\text{Ru}(\text{bpy})_3]^{3+/2+}$  couple at higher concentrations of G1.5 dendrimer is due to the effect that the surface electric field of the dendrimer generates on the solvent molecules surrounding the dendrimer surface (the species 3+ and 2+ of the redox couple are sensitive to electrostatic short-range interactions), which overcomes the effect of electrostatic long-range interactions. As expected, this effect should be more pronounced in the G4.5 dendrimer than in the G1.5 dendrimer because the surface charge density is greater in the former,<sup>33</sup> according to the results in Table 2. With regard to the  $E^{o'}$  negative shift at a fixed concentration of G1.5 dendrimer,  $4.60 \times 10^{-4} \text{ mol dm}^{-3}$ , adding increasing amounts of  $\text{Na}^+$  ion, shown also in Table 2, it seems evident that the effect of electrostatic long-range interactions for binding ruthenium(II) complex/G1.5 dendrimer is prevalent. That is, the augmenting of  $\text{Na}^+$  ions on the surface of the dendrimer cause a screening of the charge of end carboxylate groups and hence a decrease of the surface electric field, which minimizes the dielectric saturation effects.

Now ECL efficiency data can be understood. Assuming that only the free metal complex contributes to emission, if the binding of  $[\text{Ru}(\text{bpy})_3]^{2+}$ /G1.5 dendrimer was prevailing,  $\Phi_{\text{ECL}}$  should diminish with increasing dendrimer concentration because of the photoluminescence intensities not changing (see section 2.4), as happens for the case of reactions between  $[\text{Ru}(\text{phen})_3]^{2+}$  and  $[\text{Os}(\text{bpy})_3]^{2+}$  with a  $\text{C}_2\text{O}_4^{2-}$  anion in the presence of increasing amounts of calf thymus DNA.<sup>34,35</sup> On the other hand, in the presence of increasing amounts of  $\text{Na}^+$ , given that  $\text{Na}^+$  ions are located preferentially on the dendrimer surface, when its concentration increases, more species of ruthenium(II) will be free; thus, an increase in the ECL efficiency should be observed. Table 1 shows, nevertheless, augmentation in the ECL efficiency when the G1.5 dendrimer concentration increases, whereas  $\Phi_{\text{ECL}}$  values drop off with

increasing concentrations of  $\text{Na}^+$  ion. That is, trends of  $\Phi_{\text{ECL}}$  values are opposite to those expected if binding of the ruthenium(II) complex/G1.5 dendrimer is taken into account, and thus this effect does not control the ECL efficiency in the G1.5 dendrimer. For the case of the G4.5 dendrimer, however, the binding of  $[\text{Ru}(\text{bpy})_3]^{2+}$ /G4.5 dendrimer, through electrostatic short-range interactions, is prevalent because of diminishing  $\Phi_{\text{ECL}}$  values with increasing dendrimer concentration, in agreement with other results in DNA.<sup>34,35</sup>

Going back to the coreactant effect and taking into account the physical meaning of  $\Phi_{\text{ECL}}$  as previously indicated ( $\Phi_{\text{ECL}}$  is a measure of the rate constant leading to the luminescent state in relation to all of those rate constants of the homogeneous reactions involved in a given ECL mechanism), the trend of  $\Phi_{\text{ECL}}$  as a function of  $\text{Na}^+$  ion concentration (see Table 1) clearly shows a negative salt effect, according to the electrostatic theory on electron-transfer reactions between ions of opposite charge ( $\Phi_{\text{ECL}}$  follows the same trend as the rate constant). That is, the coreactant effect prevails. Likewise, the ECL efficiency trend as a function of the G1.5 dendrimer concentration can be explained as the result of the electrostatic binding and coreactant effects, which act in opposite directions: the former would diminish  $\Phi_{\text{ECL}}$  and the latter would increase  $\Phi_{\text{ECL}}$  when the concentration of the G1.5 dendrimer rises, and the coreactant effect prevails.

## 5. CONCLUSIONS

ECL efficiencies and standard formal potentials of the ruthenium(II) complex have been determined in several solutions of PAMAM G1.5 and G4.5 dendrimers. The remarkable find was that G1.5 and G4.5 dendrimers behaved as coreactants. The trends of the redox potentials show that the electrostatic (long-range and short-range) interactions are operative for binding of the ruthenium(II) complex/G1.5 dendrimer, although the coreactant effect is prevalent for the case of ECL efficiency values. In contrast, for binding of the ruthenium(II) complex/G4.5 dendrimer, the electrostatic short-range interactions are dominant in both redox potential and ECL efficiency values.

## ■ ASSOCIATED CONTENT

### 📄 Supporting Information

CV for a  $[\text{Ru}(\text{bpy})_3]^{3+/2+}$  couple and a background experiment: CV and ECL intensity as a function of time. This material is available free of charge via the Internet at <http://pubs.acs.org>.

## ■ AUTHOR INFORMATION

### ✉ Corresponding Author

\*E-mail: [pptejeda@us.es](mailto:pptejeda@us.es). Tel: +34954557175. Fax: +34954557174.

### 📄 Notes

The authors declare no competing financial interest.

## ■ ACKNOWLEDGMENTS

This work was financed by the DGICYT (Grant CTQ 2008-00008/BQU) and the Consejería de Educación y Ciencia de la Junta de Andalucía.

## ■ REFERENCES

- (1) Astruc, D.; Boisselier, E.; Ornelas, C. *Chem. Rev.* **2010**, *110*, 1857–1959.

- (2) (a) Frost, T.; Margerum, L. D. *Macromolecules* **2010**, *43*, 1218–1226. (b) Gopidas, K. R.; Lehenny, A. R.; Caminati, G.; Turro, N. J.; Tomalia, D. A. *J. Am. Chem. Soc.* **1991**, *113*, 7335–7342. (c) Tomalia, D. A.; Naylor, A. M.; Goddard, W. A., III. *Angew. Chem., Int. Ed.* **1990**, *29*, 138–175.
- (3) Beezer, A. E.; King, A. S. H.; Martin, I. K.; Mitchel, J. C.; Twyman, L. J.; Wain, C. F. *Tetrahedron* **2003**, *59*, 3873–3880.
- (4) Bhadra, D.; Bhadra, S.; Jain, S.; Jain, N. K. *Int. J. Pharm.* **2003**, *257*, 111–124.
- (5) Tekade, R. K.; Kumar, P. V.; Jain, N. K. *Chem. Rev.* **2009**, *109*, 49–87.
- (6) Buczkowski, A.; Sekowskib, S.; Gralaa, A.; Paleczb, D.; Milowskab, K. *Int. J. Pharm.* **2011**, *408*, 266–270.
- (7) Cakara, D.; Kleimann, J.; Borkovec, M. *Macromolecules* **2003**, *36*, 4201–4207.
- (8) Niu, Y.; Sun, L.; Crooks, R. M. *Macromolecules* **2003**, *36*, 5725–5731.
- (9) Duijvenbode, R. C.; Rajanayagam, A.; Koper, G. J. M.; Baars, M. W. P. L.; de Waal, B. F. M.; Meijer, E. W.; Borkovec, M. *Macromolecules* **2000**, *33*, 46–52.
- (10) Nagatani, H.; Sakamoto, T.; Torikai, T.; Sagara, T. *Langmuir* **2010**, *26*, 17686–17694.
- (11) Turro, C.; Niu, S.; Bossmann, S. H.; Tomalia, D. A.; Turro, N. J. *J. Phys. Chem.* **1995**, *99*, 5512–5517.
- (12) Liu, Y.; Bryantsev, V. S.; Diallo, M. S.; Goddard, W. A., III. *J. Am. Chem. Soc.* **2009**, *131*, 2798–2799.
- (13) Richter, M. M. *Chem. Rev.* **2004**, *104*, 3003–3036.
- (14) Miao, W. *Chem. Rev.* **2008**, *108*, 2506–2553.
- (15) (a) Zhou, M.; Robertson, G. P.; Roovers, J. *Inorg. Chem.* **2005**, *44*, 8317–8325. (b) Li, M.-J.; Chen, Z.; Zhu, N.; Yam, V. W.-W.; Zu, Y. *Inorg. Chem.* **2008**, *47*, 1218–1223. (c) Stagni, S.; Palazzi, A.; Zacchini, S.; Ballarin, B.; Bruno, C.; Marcaccio, M.; Paolucci, F.; Monari, M.; Carano, M.; Bard, A. J. *Inorg. Chem.* **2006**, *45*, 695–709. (d) Joshi, T.; Barbante, G. J.; Francis, P. S.; Hogan, C. F.; Bond, A. M.; Gasser, G.; Spiccia, L. *Inorg. Chem.* **2011**, *50*, 12172–12183. (e) Joshi, T.; Barbante, G. J.; Francis, P. S.; Hogan, C. F.; Bond, A. M.; Gasser, G.; Spiccia, L. *Inorg. Chem.* **2012**, *51*, 3302–3315.
- (16) (a) Rubinstein, I.; Bard, A. J. *J. Am. Chem. Soc.* **1981**, *103*, 512–516. (b) Kanoufi, F.; Bard, A. J. *J. Phys. Chem. B* **1999**, *103*, 10469–10480.
- (17) (a) Staffilani, M.; Eva Höss, E.; Giesen, U.; Schneider, E.; Hartl, F.; Josel, H.-P.; De Cola, L. *Inorg. Chem.* **2003**, *42*, 7789–7798. (b) Zhou, M.; Roovers, J. *Macromolecules* **2001**, *34*, 244–252. (c) Lee, D. N.; Park, H. S.; Kim, E. H.; Jun, Y. M.; Lee, J.-Y.; Lee, W.-Y.; Kim, B. H. *Bull. Korean Chem. Soc.* **2006**, *27*, 99–105. (d) Lee, D. N.; Kim, J. K.; Park, H. S.; Jun, Y. M.; Hwang, R. Y.; Lee, W.-Y.; Kim, B. H. *Synth. Met.* **2005**, *150*, 93–100. (e) Sun, F.; Chen, F.; Fei, W.; Sun, L.; Wu, Y. *Sens. Actuators B* **2012**, *170*, 702–707. (f) Lu, C.; Wang, X.-F.; Xu, J.-J.; Chen, H.-Y. *Electrochem. Commun.* **2008**, *10*, 1530–1532. (g) Jie, G.; Yuan, J.; Zhang, J. *Biosens. Bioelectron.* **2012**, *31*, 69–76. (h) Jie, G.; Yuan, J.; Huang, T.; Zhao, Y. *Electroanalysis* **2012**, *24*, 1220–1225. (i) Jie, G.; Wang, L.; Yuan, J.; Zhang, S. *Anal. Chem.* **2011**, *83*, 3973–3880. (j) Venkatanarayanan, A.; Crowleya, K.; Lestini, E.; Keyesa, T. E.; Rusling, J. F.; Forster, R. J. *Biosens. Bioelectron.* **2012**, *31*, 233–239. (k) Ma, F.; Zhang, Y.; Qi, H.; Gao, Q.; Zhang, C.; Miao, W. *Biosens. Bioelectron.* **2012**, *32*, 37–42.
- (18) Gonzalez-Velasco, J. *J. Phys. Chem.* **1988**, *92*, 2202–2201.
- (19) (a) Maness, K. M.; Bartelt, J. E.; Wightman, R. M. *J. Phys. Chem.* **1994**, *98*, 3993–3998. (b) Knight, A. W. *Trends Anal. Chem.* **1999**, *18*, 47–62.
- (20) Fan, F. R. F. *Electrogenerated Chemiluminescence*; Bard, A. J., Ed.; Marcel Dekker: New York, 2004; Chapter 2.
- (21) Mussell, R. D.; Nocera, D. G. *J. Am. Chem. Soc.* **1988**, *110*, 2764–2772.
- (22) Kapturkiewicz, A. *Electrogenerated Chemiluminescence*; Bard, J. A., Ed.; Marcel Dekker: New York, 2004; Chapter 4.
- (23) Xue Bo, Y.; Bei Bei, S.; Xi Wen, H. *Sci. China, Ser. B: Chem.* **2009**, *52*, 1394–1401.
- (24) Lopes-Costa, T.; Lopez-Cornejo, P.; Villa, I.; Perez-Tejeda, P.; Prado-Gotor, R.; Sanchez, F. *J. Phys. Chem. A* **2006**, *110*, 4196–4201.
- (25) Sanchez-Burgos, F.; Galan, M.; Dominguez, M.; Perez-Tejeda, P. *New J. Chem.* **1998**, 907–911.
- (26) It is known that tertiary amines produce ECL (see, for example, refs 13–15 and 17). Thus, tertiary amines of the PAMAM dendrimers could also contribute to the ECL emission. However, in line with section 1, the tertiary amines inside of the G1.5 and G4.5 dendrimers are entirely protonated at pH 6.1; thus, on the average, the ruthenium(II) complex species would be repelled from inside the dendrimers. Even so, some experiments were done in the presence of the G2.0 PAMAM dendrimer at pH values 6.1 and 8 (0.1 mol dm<sup>-3</sup> NaCl included). At pH 6, a weak ECL emission was observed ( $\Phi_{\text{ECL}} \approx 0.008$ ), but this one was not observed at pH 8. These facts indicate that tertiary amine groups are not responsible for the ECL spectrum in G2.0 dendrimer, but rather the end primary amine groups [when these -NH<sub>2</sub> groups are entirely protonated (at pH 8), the ruthenium(II) complex species are repelled]. Therefore, in our opinion, the end carboxylate groups of the G1.5 and G4.5 dendrimers are responsible for ECL emissions and not the tertiary amine groups inside of dendrimers.
- (27) De la Vega, R.; Perez-Tejeda, P.; Prado-Gotor, R.; Lopez-Cornejo, P.; Jimenez, R.; Perez, F.; Sanchez, F. *Chem. Phys. Lett.* **2004**, *298*, 82–86.
- (28) Kulczynska, A.; Frost, T.; Margerum, L. D. *Macromolecules* **2006**, *39*, 7372–7377.
- (29) Kulczynska, A.; Johnson, R.; Frost, T.; Margerum, L. D. *J. Chem. Educ.* **2001**, *88*, 801–805.
- (30) Neto-Ponce, P.; Sanchez, F.; Perez, F.; Garcia-Santana, A.; Perez-Tejeda, P. *Langmuir* **2001**, *17*, 980–987.
- (31) Sanchez, F.; Lopez-Lopez, M.; Perez-Tejeda, P. *Langmuir* **1998**, *14*, 3762–3766.
- (32) Ohsawa, Y.; Shimazaki, Y.; Aoyagui, S. *J. Electroanal. Chem.* **1980**, *114*, 235–246.
- (33) Turro, N. J.; Barton, J. K.; Tomalia, D. A. *Acc. Chem. Rev.* **1991**, *24*, 332–340.
- (34) Carter, M. T.; Bard, J. A. *Bioconjugate Chem.* **1990**, *1*, 257–263.
- (35) Rodriguez, M.; Bard, J. A. *Anal. Chem.* **1990**, *62*, 2658–2662.